Effect of Crystal Structure on Hydrogen Diffusivity in Zirconium Using a Machine Learning Potential

Seong-been Lee, Takuji Oda*

Department of nuclear engineering, Seoul National Univ., 1 Gwank-ro, Gwanak-gu, Seoul 08826

*Corresponding author: oda@snu.ac.kr

*Keywords: Zirconium; Hydrogen diffusion; Machine-learning interatomic potential; Atomistic simulation

1. Introduction

Zirconium alloys serve as core structural and cladding materials water-cooled reactors. where in corrosion-induced hydrogen uptake, transport, and hydride precipitation affect dimensional stability and integrity. Accurate prediction of hydrogen diffusivity (D) is therefore important. While extensive measurements exist for α -Zr (hcp), their scatter introduces uncertainty, and diffusion anisotropy remains insufficiently understood. For β-Zr (bcc), high-temperature experiments remain challenging, and only limited data are available. A computational framework that delivers phase-consistent kinetics across α and β is thus desirable.

Atomistic modeling of H migration has traditionally relied on density-functional theory (DFT) or empirical interatomic potentials. DFT provides reliable formation energetics and migration barriers; however, it becomes prohibitively expensive for long-time potential simulation. **Empirical** models enable large-scale molecular dynamics (MD); however, it often struggles to reproduce the subtle difference of formation energies between different sites, such as tetrahedral (T) and octahedral (O) sites, and the anisotropic transport tensor in α-Zr, leading to inconsistent activation energies or incorrect mechanistic pictures.

Machine-learning interatomic potentials (MLIPs) bridge this gap by fitting to diverse DFT reference data while retaining efficiency of empirical potentials. Among proposed MLIP formalisms, the moment tensor potential (MTP) has shown strong performance for multi-component metallic systems and defect-mediated kinetics. However, a compact/unified assessment of hydrogen transport in zirconium that (i) validates migration pathways against DFT and (ii) quantifies diffusivity in both α and β using the same MLIP under a consistent workflow remains limited in the literature.

This study applies a DFT-trained MTP for the Zr–H system to identify how the crystal lattice affects hydrogen diffusivity. We analyze migration pathways using the nudged elastic band (NEB) calculations and compute hydrogen diffusivity via Einstein relation analysis from MD in α -Zr (600–1000 K) and β -Zr (1200–2000 K). This study focus on the dilute-hydrogen limit, and the effects of hydrogen concentration and lattice strains are not considered.

2. Methods

2.1 Potential model construction

A moment tensor potential was fitted to a DFT reference dataset spanning both α and β zirconium phases. The reference structures included bulk α-Zr and β-Zr, dilute hydrogen interstitials in T and O sites, and configurations with applied strains or thermal perturbations. All DFT calculations were performed VASP under the generalized using gradient approximation (PBE functional). A plane-wave cutoff of 500 eV and projector-augmented-wave pseudopotentials were used, treating zirconium with 12 valence electrons $(4s^2 4p^6 5s^2 4d^2)$. Brillouin zone integrations employed Γ centered k-point meshes chosen to achieve meV-level total energy convergence. The MTP was trained by minimizing a loss function over energies, forces, and stresses, and the final model was selected based on crossvalidation against a test set.

The fitted potential reproduces fundamental properties of zirconium within typical DFT uncertainty. Specifically, the equilibrium lattice parameters and elastic constants of both α -Zr and β -Zr are captured with good accuracy [1,2]. It also correctly predicts the site preference of hydrogen in α -Zr, where the T site is more stable than the O site, consistent with DFT. As a validation of kinetic properties, NEB calculations using the MTP for representative T-O hops in α -Zr produced energy barriers in close agreement with corresponding DFT results and preserved the correct ordering of migration energies. This agreement indicates that the constructed potential is suitable for simulating finite-temperature hydrogen diffusion.

2.2 NEB and diffusion pathways

The NEB method was employed to determine minimum-energy pathways for hydrogen migration. In this approach, a series of intermediate images between fully relaxed initial and final states is optimized simultaneously, with spring forces linking the images to maintain a continuous path. We used the climbing-image NEB variant to accurately locate the highest-energy saddle point along each path. The optimization of each band proceeded until the forces on the images were negligible and the saddle-point energy converged.

For α -Zr, we focused on hops between nearest-neighbor interstitial sites. Three elementary migration events that form the three-dimensional diffusion network

were evaluated: tetrahedral-to-tetrahedral (T-T), tetrahedral-to-octahedral (T-O), and octahedral-to-octahedral (O-O) jumps. For each case, the initial and final configurations with a hydrogen atom occupying the respective sites were fully relaxed, and several intermediate images were interpolated between them. NEB calculations then yielded the energy barrier for each hop from the converged climbing-image result. The relative barrier heights confirm the T-O-T sequence as the operative long-range diffusion mechanism in α -Zr, and these elementary hops provide the basis for interpreting the MD diffusion coefficients later.

 β -Zr is only stable at elevated temperatures, and the ideal β -phase lattice (bcc lattice) at 0 K is not stable. This makes direct NEB calculations in the β phase unreliable. Therefore, we limited the explicit pathway calculations to α -Zr. Hydrogen diffusion in β -Zr was instead characterized solely through MD simulations, as described below.

2.3 Molecular Dynamics for Diffusion Coefficients

Hydrogen diffusion coefficients were computed from MD trajectories using the Einstein relation, which relates the diffusion coefficient to the linear growth of the mean squared displacement (MSD) of a diffusing particle over time. Simulations were performed on supercells representative of the dilute hydrogen limit (a $6\times6\times4$ α -Zr supercell or a 5×5×5 β-Zr supercell, each containing a single H interstitial). The temperature range was 600-1000 K for α -Zr and 1200–2000 K for β -Zr. At each temperature, 100 independent MD trajectories were generated with different initial velocity seeds. The MSD of the hydrogen atom was tracked over time in each trajectory, and diffusion coefficients were obtained by fitting the MSD vs. time curve to a linear slope. The final reported diffusivity at each temperature is the average of the 100 independent trajectory results.

3. Results and Discussion

3.1 Site stability and migration path analysis by NEB

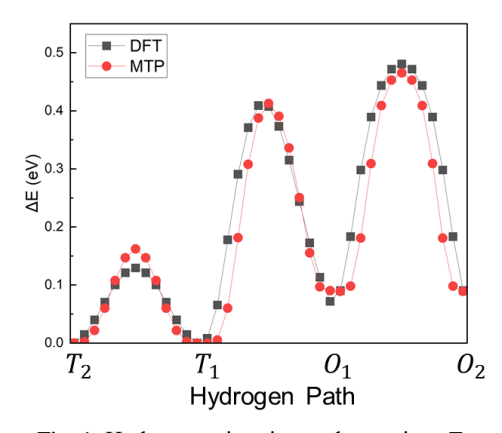


Fig. 1. Hydrogen migration pathways in α -Zr.

Figure 1 compares the computed hydrogen migration energy profile along a representative T_2 – T_1 – O_1 – O_2 path in α -Zr, as obtained from DFT and from the MTP. The subscript indicates different sites. Both DFT and MTP predict stable energy minima when hydrogen occupies T sites, with a shallower metastable well when it is at an O site. Two high-energy saddle points bracket the O basin along this path, whereas the in-plane segment connecting two T sites is associated with a much lower barrier. This ordering of energy barriers confirms that long-range diffusion proceeds via a T–O–T sequence.

The MTP-generated energy profile closely follows the DFT profile across the entire pathway, reproducing the locations of minima and saddle points and even matching the curvature around these features. Minor discrepancies appear only near the highest saddle. Because the MTP preserves the correct energy landscape and barrier ordering, the rate-limiting step for diffusion is identified as the hydrogen hopping into O site (rather than the easier in-plane T hop). This expectation is borne out by the activation energy obtained later from the MD results (see Section 3.2).

The energy landscape also sheds light on the weak diffusion anisotropy in α -Zr. While the easiest individual hops occur within the basal plane, achieving three-dimensional transport requires the involvement of an out-of-plane (O-mediated) jump, which increases the overall activation energy. We furthermore observed that applying small elastic strains (either isotropic or along specific directions) causes smooth and continuous changes in the relative stability of T vs. O sites and in the corresponding saddle point energies. The MTP is able to track these strain-induced shifts, indicating that the potential remains predictive under modest lattice distortions [3].

3.2 Diffusion in α-Zr

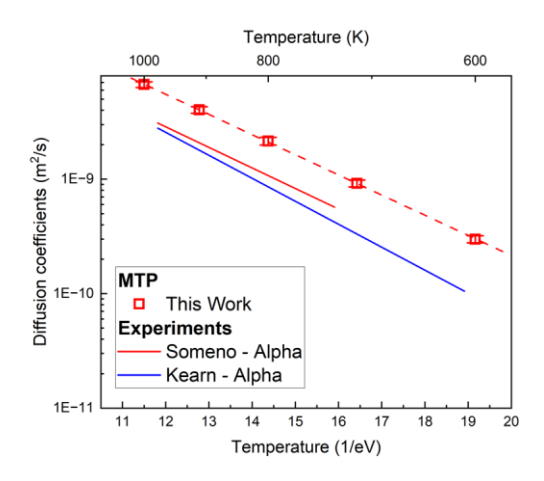


Fig. 2. Hydrogen diffusivity in α -Zr: MD versus experiments (Kearns [4]; Someno [5]).

Using the MTP, MD simulations from 600 K to 1000 K produced hydrogen diffusion coefficients in α -Zr that agree quantitatively with available experiments. For

example, the diffusivity is on the order of 10^{-10} m²/s at 600 K and rises to around 10^{-9} m²/s at 800 K and to $\sim 7 \times 10^{-9}$ m²/s at 1000 K. These values closely follow the single-crystal diffusivity measurements reported by Kearns [4] and lie within the broader range of historical data [5].

An Arrhenius plot of the α -Zr diffusion data yields an activation energy in excellent agreement with Kearns' single-crystal value [4]. This result indicates that the MTP accurately captures hydrogen transport kinetics in α -Zr.

3.3 Diffusion in β -Zr

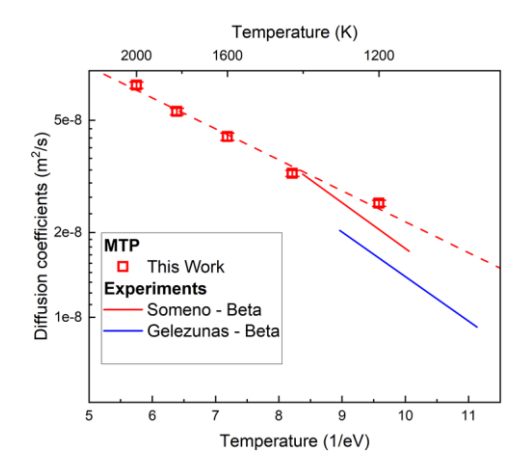


Fig. 3. Hydrogen diffusivity in β-Zr: MD versus historical measurements (Someno [5]; Gelezunas et al. [6]).

For $\beta\text{-}Zr$, hydrogen diffusion was computed from 1200 K up to 2000 K. The calculated diffusivity increases with temperature following an Arrhenius equation. For instance, the diffusion coefficient is approximately 2.5×10^{-8} m²/s at 1200 K and grows to about 6.7×10^{-8} m²/s at 2000 K (with standard errors on the order of 10^{-9} m²/s in each case). These predictions fall within the scatter of historical high-temperature diffusion measurements for $\beta\text{-}Zr$ [5,6].

3.4 Comparison of diffusivity between two phases

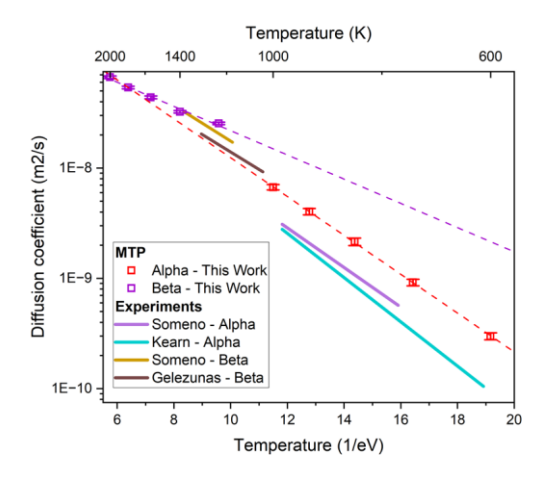


Fig. 4. Arrhenius plot of hydrogen diffusivity in α - and β -Zr.

Figure 4 compares the diffusivity in both phases with extending the temperature ranges using the Arrhenius equations. At any temperature, the β -phase regression curve lies above the α -phase regression curve, indicating a larger diffusivity for β -Zr at the same temperature. Reading off the fitted lines, the difference is already evident near 1200 K, where the diffusivity in β -Zr is approximately 3-5 times as larger as that in α -Zr; at 1400 K the gap increases to about one order of magnitude. The separation grows with temperature because the α -phase fit has a steeper negative slope, which signifies a larger activation energy for hydrogen diffusion in α -Zr (~0.4 eV) than in β -Zr (~0.25 eV).

4. Conclusions

The MTP trained on DFT accurately reproduces hydrogen migration pathways and diffusivity in both α -Zr and β -Zr. The diffusivities and activation energy of α -Zr align with single-crystal measurements, while β -Zr values from 1200–2000 K sit within the spread of historical data. A comparison between the two phases shows that the β -phase has higher hydrogen diffusivity and a lower migration barrier than the α -phase. Future work will assess the effects of hydrogen concentration and lattice strain on hydrogen diffusivity.

Acknowledgment

This research was supported by the National Research Council of Science & Technology(NST) grant by the Korean government (MSIT) (No. GTL24031-100).

REFERENCES

- [1] J. Goldak, L. T. Lloyd, C. S. Barrett, "Lattice parameters, thermal expansions, and Grüneisen coefficients of zirconium from 4.2 to 1130 K," Phys. Rev., vol. 144, no. 2, pp. 478–484, 1966, doi: 10.1103/PhysRev.144.478.
- [2] A. Heiming, W. Petry, J. Cockcroft, J. Trampenau, W. Miekeley, "The temperature dependence of the lattice parameters of pure BCC Zr and BCC Zr–2 at.% Co," J. Phys.: Condens. Matter, vol. 4, no. 3, pp. 727–733, 1992, doi: 10.1088/0953-8984/4/3/012.
- [3] I. C. Njifon and E. Torres, "A first principles investigation of the hydrogen-strain synergy on the formation and phase transition of hydrides in zirconium," Acta Mater., vol. 202, pp. 222–231, 2021, doi: 10.1016/j.actamat.2020.10.030.
- [4] J. J. Kearns, "Diffusion coefficient of hydrogen in alpha zirconium, Zircaloy-2 and Zircaloy-4," J. Nucl. Mater., vol. 43, no. 3, pp. 330–338, 1972, doi: 10.1016/0022-3115(72)90065-7. [5] M. Someno, "Hydrogen absorption of zirconium and measurement of diffusion coefficient," J. Japan Inst. Met. (Nippon Kinzoku Gakkaishi), vol. 24, pp. 249–253, 1960.
- [6] V. L. Gelezunas, P. K. Conn, R. H. Price, "The diffusion coefficients for hydrogen in β-zirconium," J. Electrochem. Soc., vol. 110, no. 7, pp. 799–804, 1963.